Key innate immune components controlling intracellular infection

Benard, E.L.

Chapter 5

Phagocytosis of mycobacteria by zebrafish macrophages is dependent on the scavenger receptor Marco, a key control factor of pro-inflammatory signalling

Erica L. Benard, Stefan J. Roobol, Herman P. Spaink, Annemarie H. Meijer

Developmental and Comparative Immunology, In press

Abstract

Scavenger receptors on the cell surface of macrophages play an important role in host defence through their ability to bind microbial ligands and induce phagocytosis. Concurrently, signal transduction pathways are initiated that aid in defence mechanisms against the invading microbe. Here we report on the function of scavenger receptor Marco (*Ma*crophage *r*eceptor with *co*llagenous structure) during infection of zebrafish embryos with *Mycobacterium marinum,* a close relative of *M. tuberculosis.* Morpholino knockdown demonstrates that Marco is required for the rapid phagocytosis of *M. marinum* following intravenous infection. Furthermore, gene expression analysis shows that Marco controls the initial transient pro-inflammatory response to *M. marinum* and remains a determining factor for the immune response signature at later stages of infection. Increased bacterial burden following *marco* knockdown indicates that this scavenger receptor is important for control of *M. marinum* growth, likely due to delayed phagocytosis and reduced pro-inflammatory signalling observed under conditions of Marco deficiency.

Introduction

Scavenger receptors (SRs) comprise a large family of transmembrane cell surface glycoproteins and are mainly expressed in macrophages, dendritic cells and endothelial cells [1]. Originally these receptors were characterised by their ability to recognise and internalise modified low-density lipoproteins (LDLs), such as oxidised LDL and acetylated LDL, thereby making these susceptible to degradation [2]. For this reason they have been extensively studied in relation to development of atherosclerosis [3]. However, SRs also have many other important functions, for example in pathogen clearance, in transport of cargo within the cell, and in lipid transport [4-6].

Class A SRs in vertebrates consist of three proteins: SR-AI, SR-AII and MARCO (*ma*crophage *r*eceptor with *co*llagenous structure). SR-AI and SR-AII are both encoded by the macrophage scavenger receptor 1 (*MSR1*) gene [7] but differ in structure due to alternative splicing of the gene product. SR-AI contains a C-terminal cysteine-rich domain which is lacking in SR-AII [8]. The trimeric membrane-bound MARCO protein has short intracellular and transmembrane domains, as well as a large extracellular domain that consists of a spacer domain, a long collagenous domain, and a C-terminal scavenger receptor cysteine-rich domain (SRCR domain V) [9]. In un-inflamed tissues, expression of mouse and human *MARCO* is restricted to macrophages of the splenic marginal zone, medullary cords of the lymph nodes, and alveolar macrophages of the lung [9-11]. Under inflammatory conditions caused by bacterial infection or lipopolysaccharide (LPS) injection, *MARCO* expression can be rapidly up-regulated [12, 13] and its expression profile extends to the splenic macrophages of both red and white pulp, dendritic cells [14], and Kupfer cells in the liver [10]. Deficiency of MARCO in mouse models and patients is

linked with autoimmune diseases such as systemic lupus erythematosus (SLE), which is most likely due to its role in the binding to and clearance of apoptotic cells, which are considered to be a major source for auto-antigens [15-18]. The first indication for a role of MARCO in anti-bacterial defence was that monoclonal antibodies inhibited capturing of heat-killed bacteria by macrophages in the marginal zone areas of the spleen in mice [13].

Recent findings supporting the immunological role of MARCO in human infections are that single nucleotide polymorphisms (SNPs) in *MARCO* are associated with increased susceptibility to pulmonary tuberculosis (TB) in humans [19, 20]. *Mycobacterium tuberculosis* is the causative agent of TB, a common and frequently lethal infectious disease. After being phagocytosed by macrophages, mycobacteria are capable of inhibiting the phagosome-lysosome fusion by interfering with the Rab-controlled membrane trafficking, allowing them to reside and proliferate in a safe environment [21]. Increased phagocytic activity of *M. tuberculosis* has been observed in mouse macrophages deficient in autophagy-related gene 7 (ATG7), which display higher expression levels of *MARCO* and *MSR1* [22]. MARCO has been shown to assist in the phagocytosis of *M. tuberculosis* in mice via specific binding to the cell wall glycolipid trehalose 6,69-dimycolate (TDM) of this bacteria and to cooperate with TLR2/CD14 signalling in activating cytokine responses [23]. TDM is capable of inducing many elements of *M. tuberculosis* pathogenesis and is predicted to be present in *M. marinum*, a natural fish pathogen and a close relative of *M. tuberculosis* [24]. *M. marinum* causes an infection in zebrafish (*Danio rerio*) that shares pathological hallmarks with human TB disease, including the formation of caseating granulomas and development of latency [25, 26].

The early life stages of the zebrafish, which are transparent, have proven extremely useful to study the early events in mycobacteria-host interactions, from phagocytosis to early granuloma formation [27-30]. We have previously shown that a zebrafish homologue of *MARCO* is expressed in embryos, downstream of the transcription factor Spi1/Pu.1 that is required for myeloid cell development [31]. Furthermore, others have demonstrated expression of *marco* in macrophages and dendritic cells of adult zebrafish [32]. Here we report on a functional study of the zebrafish *marco* gene.

We demonstrate that Marco is required for the rapid phagocytosis of *M. marinum* in zebrafish and is an essential player in the establishment of an initial transient pro-inflammatory response to this pathogen. Furthermore, we show that Marco is important for mycobacterial growth control.

Materials and methods

Zebrafish husbandry

Zebrafish were handled in compliance with the local animal welfare regulations and were maintained according to standard protocols (zfin.org). The culture was approved

by the local animal welfare committee (DEC) of the University of Leiden and all protocols adhered to the international guidelines specified by the EU Animal Protection Directive 2010/63/EU. Zebrafish lines used in this study included AB/TL, *Tg(mpeg1:EGFP)*^{gl22} [33], *Tg(mpeg1:mCherry)*^{UMSF00134}, *Tg(mpeg1:Gal4-VP16)*^{gl24} [33], *Tg*(*mpx*:*GFP*)^{i114} [35], and *Tg(UAS-E1b:NTR-mCherry)*^{i149} [36]. Embryos were grown at 28.5°C in egg water (60 µg/ml Instant Ocean sea salts). For the duration of bacterial injections and imaging, embryos were kept under anaesthesia in egg water containing 200 µg/ml tricaine (Sigma-Aldrich). Embryos used for stereo fluorescence imaging were kept in egg water containing 0.003% 1-phenyl-2-thiourea (Sigma-Aldrich) to prevent melanisation.

Marco sequence and morpholino knockdown

A cDNA clone of *marco* (EST CO929777) was obtained from GenomeCube. The full length sequence was determined by the sequencing service of BaseClear (Leiden, Netherlands) and submitted to GenBank (accession number BankIt1734081 Marco KJ955494). Protein domains were detected with SMART analysis. Amino acid identity and similarity percentages were determined using UniProt CLUSTAL O(1.2.0) multiple sequence alignment. Splice blocking morpholino oligonucleotides were designed based on the alignment of the cDNA sequence with the genomic sequence from Ensembl gene ENSDARG00000059294 (Supplementary fig 1A). Two morpholinos were obtained from Gene Tools, morpholino 1 targeting the intron 15-exon 16 boundary and morpholino 2 targeting the exon 9-intron 9 boundary (Mo1: 5'ACGGACCACTGATGAAGAAAAACAA3'; 0.02 mM and Mo2: 5'TAACTAAAAGTACCTTGGCTTCCAC3'; 0.3 mM). Morpholinos were diluted to the desired concentration in 1x Danieau buffer (58 mM NaCl, 0.7 mM KCl, 0.4 mM $MgSO_4$, 0.6 mM $Ca(NO_3)_2$, 5.0 mM HEPES; pH 7.6) containing 1% phenol red (Sigma-Aldrich) and 1 nl was injected into the yolk at the 1-2 cell stage using a Femtojet injector (Eppendorf). As a control the standard control oligonucleotide from Gene Tools was used.

Chemical treatments

For nitroreductase-dependent macrophage ablation, metronidazole, (10 mM, 2 hours treatment, Sigma-Aldrich, M3761) was administered via the egg water to 3 days post fertilisation (dpf) embryos. Copper sulphate ($CuSO_4$, 10 uM, 2 hours treatment, Merck, #1027910250) was administered via the egg water to induce cell death of neuromast hair cells and a subsequent inflammatory response [37]. After copper sulphate treatment the embryos were briefly washed three times with egg water and fixed in 4% paraformaldehyde in PBS.

Infection experiments

Mycobacterium marinum infections were performed using the Mma20 strain expressing mCherry in a pSMT3 vector [38] or the *Salmonella typhimurium* strain SL1027 carrying the DsRed expression vector pGMDs3 [39]. Embryos were staged at 24 hours post fertilisation

(hpf) by morphological criteria [40] and manually dechorionated. Bacteria were prepared and injected into the blood circulation at 28 hpf [41] and PBS or 2% Polyvinylpyrrolidone (PVP40) in PBS (w/v) was used as a mock injection. In experiments for fluorescent bacterial pixel count and qPCR analysis, 200 colony forming units (cfu) of *M. marinum* was used. In experiments for phagocytosis analysis, 180 cfu *M. marinum* or *S. typhimurium* was injected into the blood circulation at 30 hpf. This stage of development was used because the Duct of Cuvier is located more laterally over the yolk sac compared to 28 hpf which facilitates imaging purposes for quantification. Infected embryos were fixed at 5, 10, 20 and 30 minutes post infection (mpi) in 4°C 4% paraformaldehyde in PBS. Leukocytes were immuno-labelled and the number of intra- and extra-cellular bacteria was counted over the yolk sac.

Fluorescence-activated cell sorting

Macrophages and neutrophils were isolated by FACS from 6 dpf *Tg(mpeg1:mCherry)^{UMSF001}* [34] and *Tg*(*mpx*:GFP)^{i114} [35] zebrafish larvae, respectively. The procedure is described in detail in [42]. In short, larvae were dechorionated using pronase treatment, rinsed in calcium-free Ringer solution, and digested with 0.25% trypsin. The obtained cell suspension was centrifuged, rinsed with PBS and resuspended in Leibovitz medium L15 without phenol red, 1% fetal calf serum, 0.8mM CaCl2, penicillin 50 U/ml and streptomycin 0.05 mg/ml. The single cell suspension was subjected to FACS at room temperature using a FACSAria (Becton Dickinson) with the BD FACSDiva software version 5.0.3 and a Coherent Sapphire solid state laser 488 nm with 13 mW power. The GFP+ and GFP- cell fractions were collected as above but with 10% fetal calf serum and RNA was isolated using the RNAaqueous Micro Kit (Ambion).

RNA isolation, cDNA synthesis, and expression analyses

Whole embryo RNA isolation, removal of residual genomic DNA, cDNA synthesis and quantitative RT-PCR (qPCR) analysis was performed as described in [43]. qPCR results were analysed using the ΔΔCt method. All reactions were performed as technical duplicates and data were normalised to the expression of peptidylprolyl isomerase A like (*ppial*) for whole embryo samples and to *eukaryotic translation initiation factor 4A, isoform 1B* (*eif4a1b*) for cells isolated by FACS. Primer sequences for *ppial* and *marco* are described in [31], primer sequences for *mmp9* and *il1b* are described in [43], and primer sequence for *eif4a1b* are: FW: 5'TTCAGAAACTCAGTACTAGCATACA3'; REV: 5'GTGACATCCAACACCTCTGC3'. Knockdown of *marco* with morpholino 1 was verified by qPCR and to validate the knockdown of morpholino 2, the SuperScript® One-Step RT-PCR System (Invitrogen, #10928-034) was used with 50ng DNAse treated RNA template. RT-PCR primers for *marco* knockdown verification were FW: 5'GACAGACAGGAGATCCTGG3'; REV: 5'CTCCACGCTCACCTTTGAGAC3'. The following adjustments were made to the PCR settings: 59.4°C for 30 seconds for the annealing step of the PCR amplification with 30 cycles.

RNA for deep sequencing analysis was isolated using QIAzol lysis reagent and purified using the Rneasy MinElute Cleanup kit (QIAGEN Benelux B.V., Venlo, Netherlands). RNA sequencing was performed as previously described [44]. Gene Expression Omnibus (GEO) database accession for RNASeq: GSE58230.

Immunohistochemistry

Identification of neutrophils and macrophages was done by immuno-labelling with a leukocyte specific L-plastin antibody and Alexa568/488-conjugated secondary antibody, combined with neutrophil specific staining for myeloperoxidase activity [45].

Imaging

Stereo fluorescence images were taken with a Leica MZ16FA stereo fluorescence microscope equipped with a DFC420C digital colour camera. Overlay images of bright field and fluorescence stereomicroscopy were made using Fiji [46]. Bacterial pixel counts were obtained on stereo fluorescence images and analysed using dedicated software [47]. Quantification of phagocytosis was performed on an Axiovert 100M microscope with a W Plan-APOCHROMAT 40x 1.0 NA objective. Confocal images were taken on a Leica TCS SPE with an HCX APO 40x 1.0 NA objective and the Nikon Ti Eclipse with a plan apo 20x NA 0.75 WD 1mm with V (violet) correction.

Statistical analysis

All data (mean ± SEM) were analysed using unpaired, two-tailed t-tests for comparisons between two groups and one-way ANOVA with Tukey's Multiple Comparison method as a post-hoc test for other data (*, $p<0.05$; **, $p<0.01$; ***, $p<0.001$).

Results

The zebrafish *marco* gene is expressed in larval macrophages and is up-regulated during infection

Sequencing of a cDNA clone of the zebrafish *marco* gene revealed that the predicted protein shows more than 60% similarity with murine and human MARCO and has a highly conserved protein domain structure (fig. 1A-C, Supplementary table 1A). The similarity is highest (ca. 85%) in the C-terminal cysteine-rich domain, which is essential for the binding of bacteria [48] (Supplementary table 1B). To confirm the expression of *marco* in macrophages of zebrafish larvae, we used a transgenic macrophage reporter line, *Tg(mpeg1:mCherry)* to isolate macrophages by FACS at 6 days post fertilisation (dpf). We found the expression of *marco* to be highly enriched in the fluorescent macrophage cell fraction compared to the fluorescent-negative background (fig. 1D). In addition, *marco* expression is lowly expressed in neutrophils sorted from 6 dpf *Tg*(*mpx*:*GFP*) transgenic larvae (fig. 1E). We previously observed that *marco* is induced during *S. typhimurium*

infection in zebrafish embryos [49], therefore, we sought to determine whether zebrafish *marco* is regulated in a similar manner during infection with *M. marinum*, the natural mycobacterial pathogen for fish. qPCR analysis showed that *marco* is induced at 4 hours post infection (hpi) (fig. 1F), however, no difference in expression level could be observed at 4 days post infection (dpi) (fig. 1G), a time point when the embryos are severely infected and contain granuloma-like structures.

Marco functions in the phagocytosis of *M. marinum*

The conserved protein domain structure of zebrafish Marco allows us to hypothesise that it functions as a phagocytic scavenger receptor, similar to mammalian MARCO. To test this hypothesis, we set up an *in vivo* assay to determine the percentage of phagocytosed *M. marinum* at various time points. The assay consists of microinjecting a single cell suspension of fluorescently labelled *M. marinum* into the blood circulation at the site of the blood island, fixing the embryos at 5, 10, 20 and 30 mpi, immuno-labelling leukocytes with L-plastin antibody [50], and counting of intra- and extra-cellular *M. marinum* at the site of the Duct of Cuvier under a fluorescence microscope (fig. 2A). Following intravenous injection *M. marinum* is phagocytosed specifically by macrophages [27, 51] and neutrophils are known to be unable to efficiently phagocytose bacteria in liquid compartments such as the blood circulation [52], Therefore, we considered the L-plastin labelled leukocytes with internalised *M. marinum* as macrophages. The Duct of Cuvier was used as the counting site because it is distant from the site of injection, thereby avoiding interfering wounding effects, and it is located close to the surface, which facilitates imaging. Two sources of *M. marinum* can be used for this assay: a glycerol stock or a 7H9 liquid culture stock grown to logarithmic phase [41]. By injecting aliquots of a glycerol stock of *M. marinum* the dose could be kept constant throughout experiments, however, the injected glycerol stock bacteria showed a faster rate of phagocytosis (97% at 30 mpi) (fig. 2B+C) compared to the liquid culture bacteria (65% at 30 mpi) (fig. 2D) in the control embryos.

We used an antisense morpholino oligonucleotide approach to block intron-exon splicing events for zebrafish *marco* (Supplementary fig 1B+C). Morpholino-mediated knockdown of *marco* did not affect leukocyte development (Supplementary fig 1D and E). The ability of leukocytes to migrate towards a local inflammation site was also not affected. This was verified by performing a chemically induced inflammation (ChIN) assay [37] in which copper-induced damage of neuromast hair cells was capable of attracting both macrophages and neutrophils in the *marco* morphants similar as in the control group (Supplementary fig 1F). Injection with equal numbers of glycerol stock bacteria in the *marco* morphants (Supplementary fig 1G) showed that the morphants showed a significant reduction in the phagocytosis of *M. marinum* (fig. 2B) at time points up to 20 min after injection. By 30 min after injection the difference was no longer significant, indicating that phagocytosis of *M. marinum* in *marco* morphants is delayed but not abolished. This delay in phagocytosis of *M. marinum* was phenocopied with a second morpholino targeting another intron-exon boundary (fig. 2C). In addition, a delay in

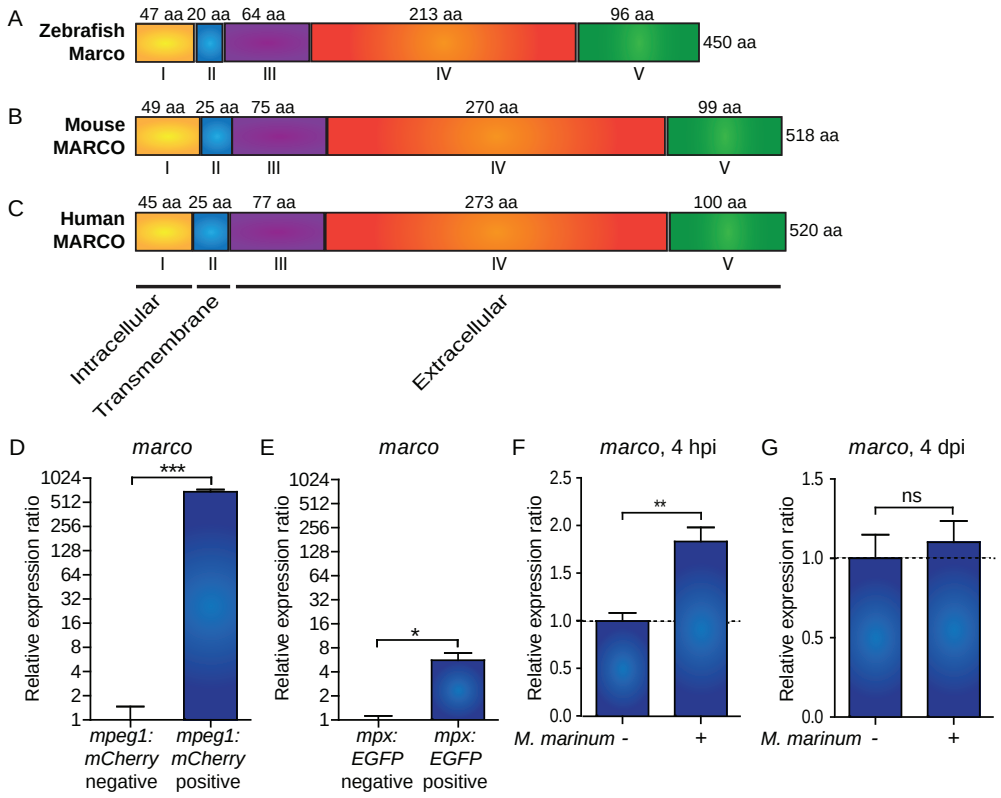

Figure 1. Zebrafish *marco* encodes a macrophage specific protein with conserved domains and is induced during early *M. marinum* infection. Comparison of the predicted (A) zebrafish Marco protein structures with (B) murine and (C) human MARCO. The cytoplasmic domain (I), transmembrane domain (II), short spacer domain (III), collagenous domain (IV), and C-terminal cysteine-rich domain (V) are conserved domains detected by SMART analysis. The domains are indicated by Roman numbers; the amino acid (aa) residue lengths of the subunit chains are indicated above their corresponding domains; and the total protein lengths are indicated to the right. The predicted cellular location of each region is indicated below. (D-E) Zebrafish *marco* is expressed in macrophages. Expression of *marco* in (D) macrophages and (E) neutrophils. qPCR analysis was performed on RNA from fluorescence-positive cell fractions obtained by cell sorting of 6 dpf larvae transgenic reporter lines for macrophages (*Tg(mpeg1:mCherry)*) and neutrophils (*Tg(mpx:EGFP)*). Expression was compared against the fluorescence-negative cell fraction of each transgenic line. (F-G) *marco* is up-regulated during early *M. marinum* infection. qPCR analysis was performed on RNA from (F) 4 hpi and (G) 4 dpi mock injected and *M. marinum* (200 cfu) injected AB/TL embryos. All graphs show data combined from three biological replicates (n=15 per group, pooled per replicate).

phagocytosis was also observed in the *marco* morphants injected with *M. marinum* from liquid culture (fig. 2A and D). In this experiment, the reduction of phagocytosis was significant at time points between 10 and 30 min after injection.

To investigate whether other scavenger receptors have a similar function in aiding phagocytosis of *M. marinum* we chose to knock down *cd36*, a class B scavenger receptor that is down-regulated during *M. marinum* infection at 4 days post infection (dpi) (data not published) and is shown to play a role in phagocytosis of bacteria such as *Staphylococcus aureus* [53]. The results showed that Cd36 does not influence the phagocytosis of *M. marinum* in zebrafish embryos (fig. 2A and E). Furthermore, in another study we similarly knocked down *mpeg1*, a different macrophage specific gene with no suggested function in phagocytosis and found that this gene also does not influence the phagocytosis of *M. marinum* [54]. To test whether Marco plays a role in the phagocytosis of other intracellular pathogens we performed the phagocytosis assay with *Salmonella typhimurium*. A significant reduction of phagocytosed bacteria was observed in *marco* morphants at 30 and 60 min post injection (Supplementary fig 2), indicating that Marco is not merely specific for phagocytosis of *M. marinum*. At 2 h post injection the complete dose of injected bacteria had been phagocytosed both in *marco* morphants and in the control embryos, indicating that Marco deficiency delays but does not abolish phagocytosis of *S. typhimurium*, similar as observed for *M. marinum* (Supplementary fig 2). Since both the scavenger receptor Cd36 and the macrophage specific Mpeg1 do not affect phagocytosis, we conclude that Marco plays a specific role in bacterial phagocytosis by macrophages.

marco knockdown has no detectable effect on the phagocytosis of ablated cells

After identifying a direct antimicrobial phagocytic function of Marco, we further sought to define whether Marco also plays a role in a different phagocytic process, namely phagocytosis of dying cells. Previous research has shown that murine MARCO is capable of binding to apoptotic cells, indicating a function in the phagocytosis and clearance of dead cells [15, 16]. Specific collective cell death at a controlled time-point can be achieved in zebrafish larvae by using nitroreductase-mediated ablation. We created a double transgenic line of *Tg(mpeg1:EGFP)* and *Tg(mpeg1:Gal4-VP16)/Tg(UAS-E1b:NTR-mCherry)* in which all macrophages express GFP and a subpopulation expresses nitroreductase mCherry. Not all GFP-positive macrophages in this line express mCherry due to silencing of the UAS promoter [55]. Cell death was induced in this subpopulation of macrophages expressing nitroreductase by treating the embryos with metronidazole, which is metabolised into a toxic product [36, 56]. At 120 minutes post treatment (mpt) the nitroreductase-positive subpopulation of macrophages started dying, between approximately 150 and 260 mpt the dead cells became phagocytosed by healthy GFP-positive macrophages, which then continued to migrate away from the site of phagocytosis between 260 and 280 mpt (fig. 3). In simultaneously time lapse recordings of 4 embryos per group, we detected 4-6 phagocytosis events in each of the *marco* morphants and control embryos (Supplementary fig 2B). Therefore, this analysis did not reveal a significant effect of *marco* knockdown on phagocytosis of chemically ablated cells.

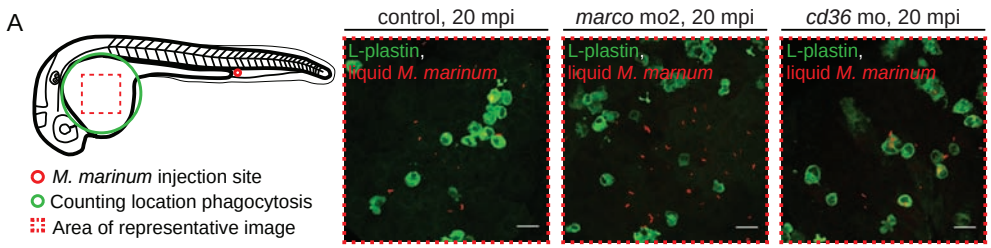
A
control, 20 mpi
marco mo2, 20 mpi
cd36 mo, 20 mpi
L-plastin,
liquid M. marinum
M. marinum injection site
Counting location phagocytosis
Area of representative image

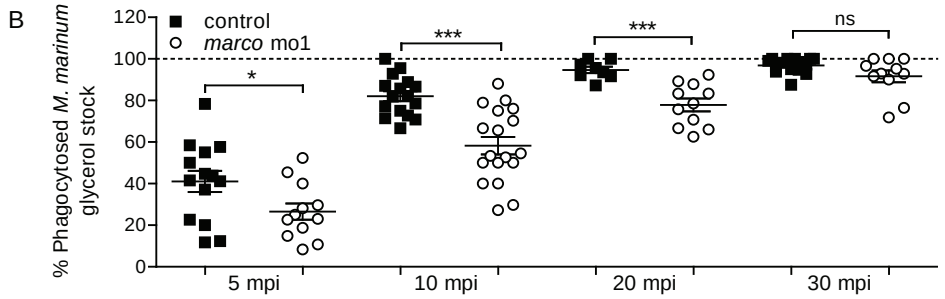
B
% Phagocytosed M. marinum glycerol stock
control
marco mo1
5 mpi
10 mpi
20 mpi
30 mpi
ns

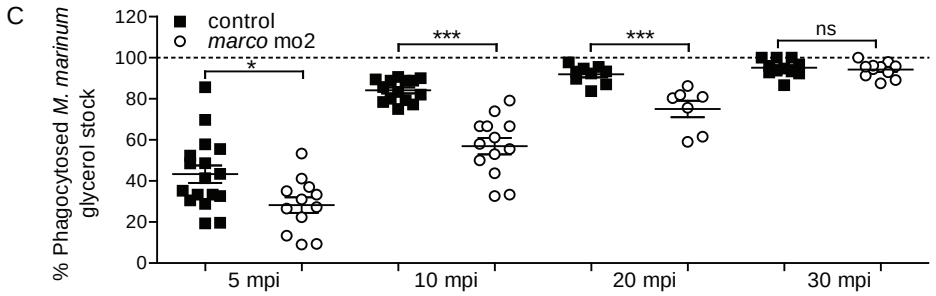
C
% Phagocytosed M. marinum glycerol stock
control
marco mo2
5 mpi
10 mpi
20 mpi
30 mpi
ns

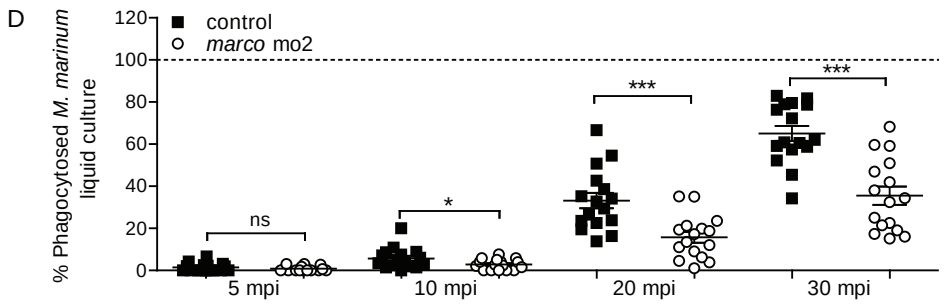
D
% Phagocytosed M. marinum liquid culture
control
marco mo2
5 mpi
10 mpi
20 mpi
30 mpi
ns

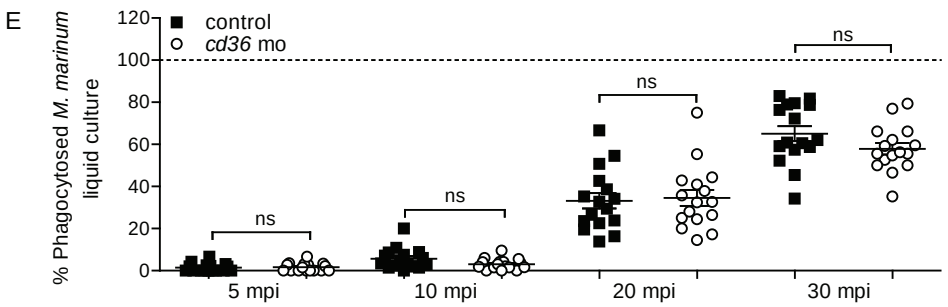
E
% Phagocytosed M. marinum liquid culture
control
cd36 mo
5 mpi
10 mpi
20 mpi
30 mpi
ns

Figure 2. Marco functions in the phagocytosis of *M. marinum*. Quantification of *M. marinum* phagocytosis. (A) Schematic overview of the phagocytosis quantification process and representative images of infected control embryos, *marco* morphants (mo2), and *cd36* morphants at 20 mpi. (B-D) Morphants of *marco* ((B) morpholino 1 and (C-D) morpholino 2) show a delayed phagocytosis of *M. marinum* (B-C) glycerol stock and (D) 7H9 liquid culture. (E) Morphants of *cd36* show no difference in phagocytosis of *M. marinum*. Each data point represents the percentage of phagocytosed *M. marinum* in an individual embryo.

Marco is required for a pro-inflammatory response following phagocytosis of *M. marinum*

The host immune response to mycobacteria includes production of pro-inflammatory cytokines induced by TLR2 detection of pathogen-associated molecular patterns (PAMPs), and MARCO has been proposed to function cooperatively with this receptor [23]. After identifying that Marco facilitates bacterial phagocytosis, we then investigated whether zebrafish Marco also plays a role in inducing a pro-inflammatory cytokine response to *M. marinum.* Therefore, we analysed the gene expression levels of *il1b*, *il8* and *mmp9* to *M. marinum* at 4 hpi based on a time-course analysis that showed significant up-regulation of cytokine and matrix metalloproteinase gene expression in our infection model (data not shown). As expected, all the genes were significantly up-regulated in the control embryos at 4 hpi; however, upon knockdown of *marco*, these genes were no longer significantly up-regulated at this time-point (fig. 4A-C). Subsequently, we investigated whether the *marco* morphants completely lacked this pro-inflammatory response during time or whether there was merely a delay in response, similar to the delay in phagocytosis of *M. marinum*. Expression levels of *il1b* were determined every hour from 2 hpi until 6 hpi (fig. 4D). As expected, the control embryos showed significant *il1b* up-regulation, of which the peak (5-fold) was at 3 hpi in this experiment. At this time-point the *marco* morphants had a significantly lower level of *il1b* up-regulation (2-fold). After the peak at 3 hpi, the *il1b* expression response in the controls declined and became non-significant at 6 hpi. At none of the time point tested, did *marco* morphants reach the same peak level of *il1b* up-regulation as observed in the control group. This led us to conclude that Marco is an essential player in the establishment of an initial transient pro-inflammatory response to *M. marinum* infection.

Marco deficiency also leads to an altered immune response at the granuloma stage of *M. marinum* infection

Since *marco* morphants showed a reduced pro-inflammatory response in the first hours after infection, we next studied whether the morphants have a differently regulated immune response to *M. marinum* at a later stage of infection, when characteristic granulomatous lesions have formed. For this purpose we analysed RNA sequencing (RNA-Seq) profiles of pools of uninfected and infected *marco* morphants and controls at 4 dpi. Although the morpholino effect is likely to have diluted out over time, an

RNA-Seq profile at this stage should reveal if *marco* knockdown has a longer lasting effect. We had previously identified a gene set showing robust and reproducible up-regulation at this stage of the infection {Benard, In press #430}. As shown in figure 5A (and Supplementary table 2), several genes from this signature set display an altered response in infected *marco* morphants compared to infection in the control group. Under conditions of *marco* knockdown we observed a significantly higher up-regulation (2-fold or higher) of genes such as *mmp9, mmp13a, moxd1, steap4, tcap,* and *timp2b.* In addition, a non-coding RNA (*si:ch211-243g18.3*) showed approximately 20-fold higher up-regulation. Conversely, expression levels of other genes, such as *cyp1a*, *cyp24a*, and *hmox1*, appeared to be significantly lower in infected *marco* morphants compared with infected controls. The level of *il1b* up-regulation was similar in both infected groups, in contrast to the reduced up-regulation of this gene in *marco* morphants during the first hours of infection. In conclusion, at the late stage of infection, knockdown of *marco* causes an altered immune response, but pro-inflammatory signalling is not impaired.

Marco is important for mycobacterial growth control

Our observations that knockdown of *marco* (i) delays phagocytosis of *M. marinum*, (ii) suppresses the initial pro-inflammatory response to this infection, and (iii) affects the expression signature of larvae with mycobacterial granulomas, suggest that Marco contributes to controlling *M. marinum* growth. We therefore investigated the bacterial burden of *marco* morphants during *M. marinum* infection. Control embryos and *marco* morphants were infected with *M. marinum* at 28 hpf and the bacterial fluorescent pixels per embryo were analysed at 4 dpi. The results show that Marco deficiency leads to a significant increase in *M. marinum* bacterial burden (fig. 5B+D) and this effect could be verified by using a second splice-blocking morpholino of *marco* (fig. 5C+E). This increased infection level of *marco* morphants indicates that Marco plays a protective role in innate host defence against mycobacterial infection.

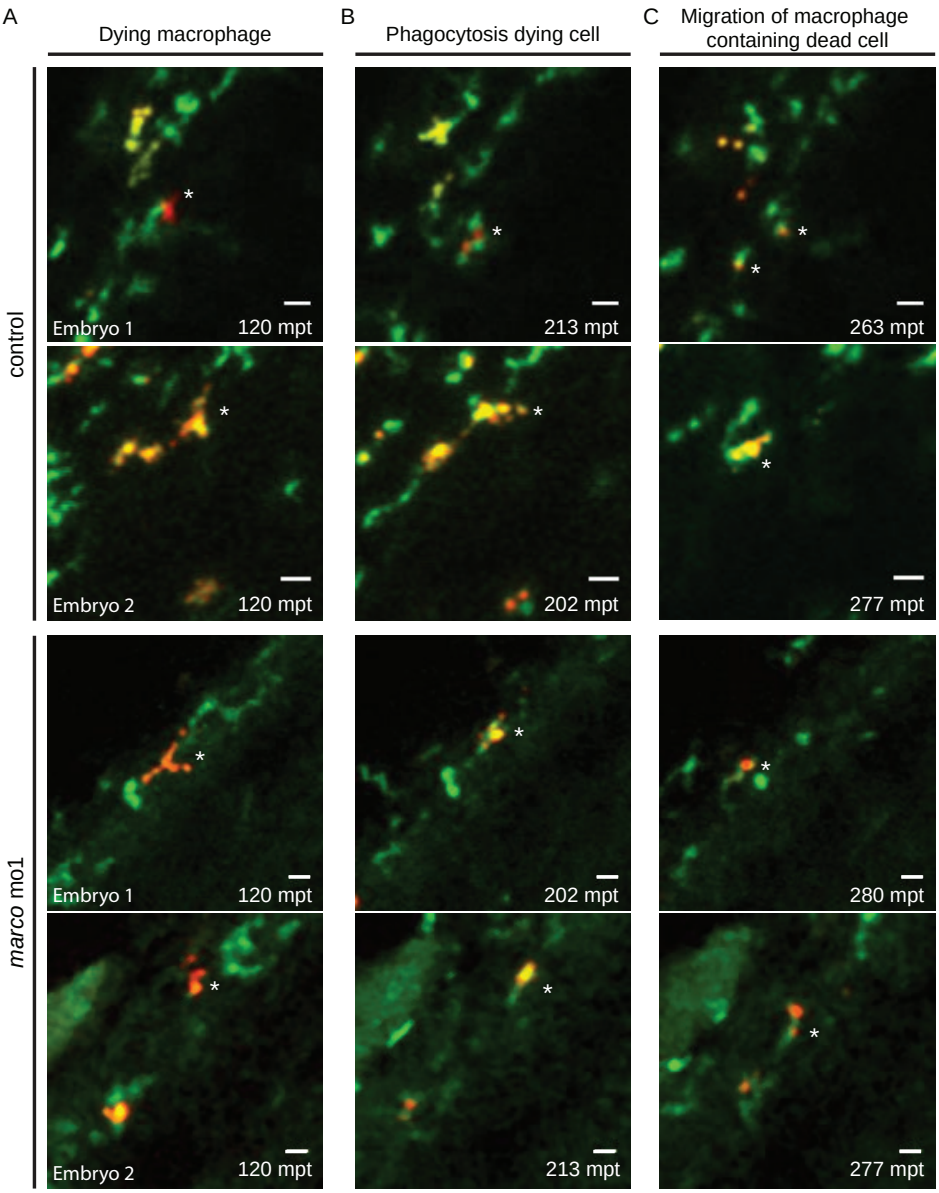

Figure 3. Morphants of *marco* are capable of phagocytosing dead cells. Phagocytosis of dying cells by macrophages was monitored in time. *marco* morphants and their controls were imaged after metronidazole treatment which induces nitroreductase-mediated cell ablation in a subpopulation of macrophages (mCherry positive cells). All macrophages express GFP. Time points represented are (A) time of nitroreductase-positive cells undergoing cell death, (B) phagocytosis of the dying cells by healthy GFP-positive macrophages and (C) migration of the macrophage containing the dead cell. Time lapse recordings were made of 4 embryos per group and examples of phagocytosis are shown for 2 control embryos en 2 *marco* morphants. Quantification of phagocytosis events are shown in Supplementary fig 2B. Asterisks indicate the phagocytosing macrophage; mpt: minutes post treatment.

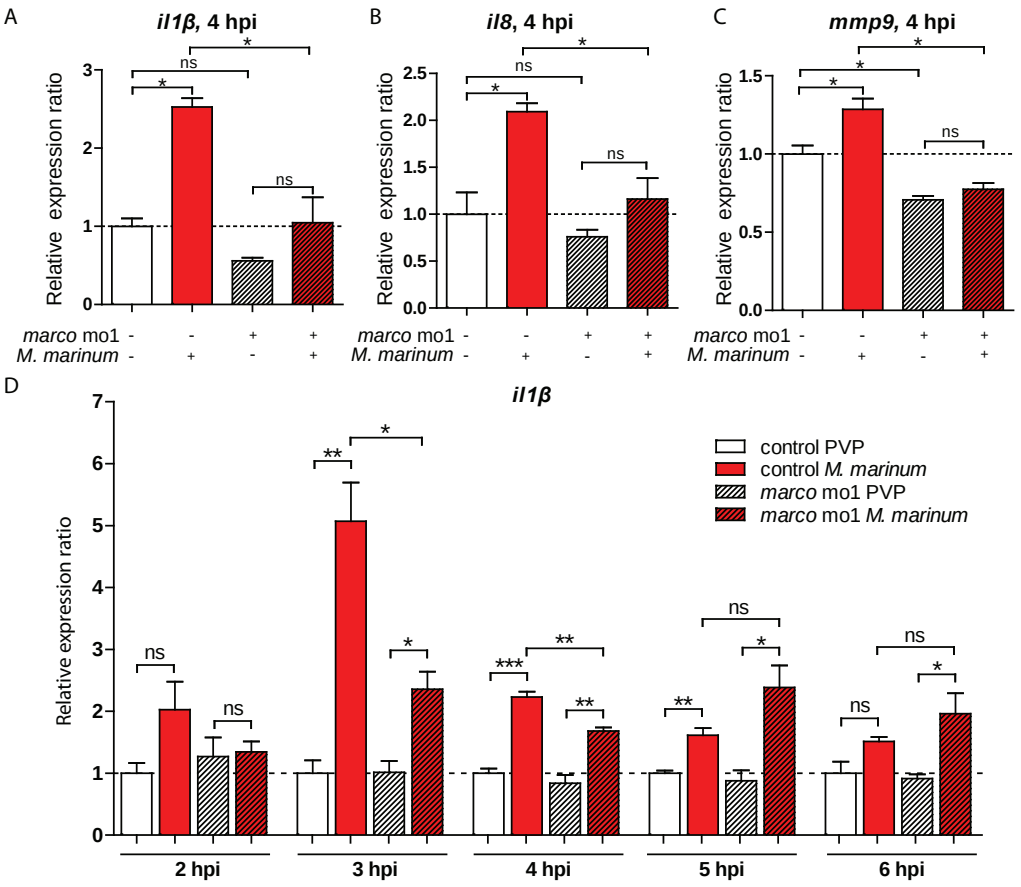

Figure 4. Morphants of *marco* have suppressed induction of pro-inflammatory cytokine response to *M. marinum*. (A-C) Effect of *marco* knockdown on the response of *il1b*, *il8* and *mmp9* to *M. marinum* infection. Expression levels of (A) *il1b*, (B) *il8* and (C) *mmp9* were determined by qPCR for marco morphants and their control embryos at 4 hpi after infection with *M. marinum* (200 cfu) and mock PVP injected controls; (D) Effect of *marco* knockdown on *il1b* expression in time (2-6 hpi). Expression was compared against the control PVP sample of each time point. All graphs show data combined from three biological replicates (n=15 per group, pooled per replicate).

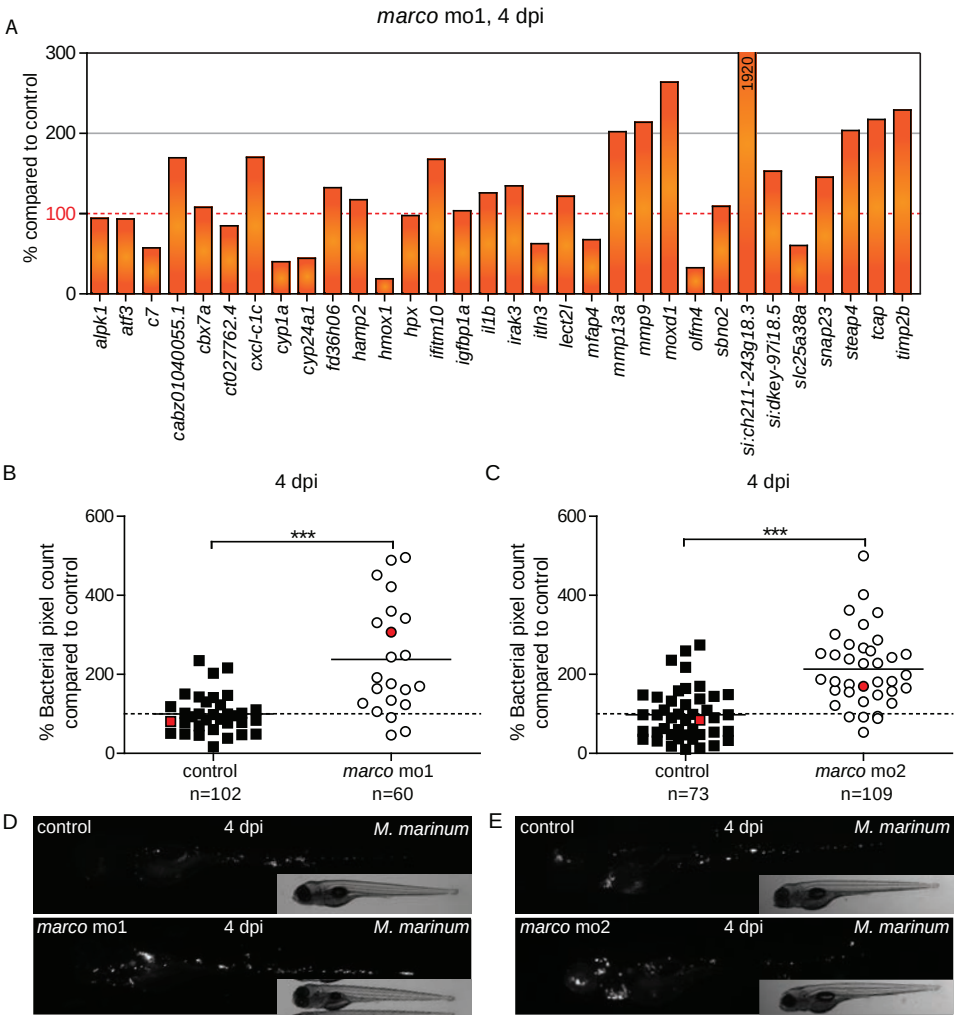

Figure 5. Effect of *marco* knockdown on the innate immune response and control of *M. marinum* infection. (A) Graph of the percentage of expression levels of infected *marco* mo1 morphants compared to infected control embryos on a set of 32 genes that showed reproducible induction by *M. marinum* infection in control embryos. The expression level of these genes under conditions of *marco* deficiency is expressed as the percentage of the expression level in the corresponding control. Results are based on RNA-Seq analysis of pools of 30 infected and 30 uninfected embryos for each group. Embryos were injected with *M. marinum* (200 cfu) or mock injected with 2% PVP, and RNA-Seq analysis was performed at 4 dpi. (B-E) *marco* knockdown impairs control of *M. marinum* infection. AB/TL embryos were injected with two different splice blocking morpholinos against (A-D) *marco* or with control morpholino, subsequently injected with mCherry-expressing *M. marinum*, and infected embryos were imaged at 4 dpi. (B-C) Bacterial burden was quantified by determining the number of fluorescent bacterial pixels and (D-E) representative stereo fluorescent images are shown below the graph of each experiment. Red symbols indicate which individuals are shown below as representative images. Graphs show combined results of 3 repeated independent experiments. Each data point represents an individual embryo.

Discussion

Phagocytosis of bacteria is an essential host defence mechanism carried out by macrophages and scavenger receptors are a key component of this process. MARCO is a scavenger receptor that has been shown to bind the cell wall component TDM of *M. tuberculosis* [23]. Here we have used a zebrafish model for tuberculosis and show that Marco mediates phagocytosis of *M. marinum* and that the initial pro-inflammatory response to this infection is dependent on Marco. We also observed a higher bacterial burden of *M. marinum* infection under conditions of *marco* knockdown.

M. marinum circulating in the blood of zebrafish embryos is rapidly phagocytosed by macrophages [57]. When *marco* was knocked down with a targeted morpholino oligonucleotide approach we observed a delay in phagocytosis of *M. marinum*. Similarly, we found that phagocytosis of intravenously injected *S. typhimurium* bacteria is also delayed under *marco* knockdown conditions. This *M. marinum* phagocytosis delay is specific for *marco* deficiency because it was repeatedly observed with two morpholinos targeting different exon-intron boundary sites and knockdown of control genes *cd36*, encoding a class B scavenger receptor, and *mpeg1,* encoding a macrophage-specific perforin*,* has no effect on phagocytosis. That *marco* deficiency does not completely abolish phagocytosis was not unexpected. One explanation might be that we used morpholinos, which generally produce a partial knockdown. A second explanation is that there are multiple receptors that can initiate phagocytosis of mycobacteria, such as the complement receptors (CRs) CR1, CR3, and CR4 that phagocytose opsonised *M. tuberculosis* [58-60], and the mannose receptors that interact with lipoarabinomannan (LAM) in the mycobacterial cell wall [61, 62]. Therefore, it is remarkable that knockdown of a single scavenger receptor, Marco, causes a significant delay in the phagocytosis of *M. marinum*. This indicates that apparently other receptors cannot fully compensate for the reduction of Marco.

When trying to establish whether Marco also plays a role in the phagocytosis of apoptotic or necrotic macrophages infected with *M. marinum*, we found image quantification of this process extremely difficult due to the sporadic occurrence and the varying location of these events. This prompted us to create an inducible system in which we could provoke cell death of a subpopulation of macrophages. Using this system, we found no evidence for a function of Marco in phagocytosis of dead cells resulting from toxification. However, it is possible that a null mutant of *marco,* which is currently not available, might reveal a stronger phenotype. Furthermore, we cannot exclude that Marco may still play a scavenging role during infection-induced cell death.

Studies using macrophages isolated from MARCO$^{-/-}$ mice have demonstrated that MARCO is preferentially utilised to "tether" mycobacterial TDM to the macrophage and to activate the TLR2 signalling pathway in response to this virulence factor [23]. This signalling not only requires MARCO and TLR2 but also CD14, which functions as a co-receptor.

CD14 is suggested to enhance the physical proximity of bacterial lipopeptides to the TLR1/2 heterodimers, without binding directly to the receptor complex [63-65]. However, CD14 alone cannot facilitate the TLR1/2-mediated response to bacterial lipopeptides because an additional co-receptor, such as MARCO, is needed [23]. Macrophages from MARCO-/- mice also produced markedly lower levels of pro-inflammatory cytokines in response to infection with virulent *M. tuberculosis*. In addition, MARCO has been shown to function in the non-opsonic recognition of *Streptococcus pneumoniae*, which leads to increased Nod2- and TLR2/CD14-dependent chemokine and cytokine production and, ultimately, the recruitment of effector monocytes/macrophages [4]. Here we confirm the finding that Marco functions as an essential player in the establishment of a pro-inflammatory response to mycobacteria in an *in vivo* infection model. However, the accessory molecule CD14 that is shown to interact with MARCO during this signalling process in mice, does not exist in the zebrafish genome [66]. Our results therefore indicate that zebrafish Marco is capable of functioning independently of the co-receptor CD14 in mediating a pro-inflammatory response to *M. marinum*. Since Tlr2 is conserved within fish and is capable of recognising (myco)bacterial ligands [67, 68], it is still likely that Marco functions as a co-receptor of Tlr2 in the recognition and phagocytosis of *M. marinum*.

Conclusion

Other interactions between scavenger receptors and TLR signalling are also known. Macrophages of mice have been shown to up-regulate *Marco* via LPS-induced TLR4 signalling, which can be a mechanism to increase phagocytic activity [69]. Similarly, when we infect zebrafish with *S. typhimurium*, an LPS-containing pathogen, we observe induction of *marco* [49]. In the present study, we have demonstrated that *marco* is also induced during the early stage (4 hpi) of *M. marinum* infection. The up-regulation of *marco* at this stage coincides with the time point during which the host produces a Marco-dependent pro-inflammatory response to *M. marinum*.

In this study we show that Marco is important for rapid phagocytosis of *M. marinum*, a process that most likely reoccurs during the development of granuloma-like structures when bacteria are released from necrotic cells. Marco is also is essential for the maximum induction of the initial pro-inflammatory response towards *M. marinum* infection, and remains a determining factor for the immune response signature at later stages of infection. All these factors probably contribute to the fact that *marco* deficiency leads to increased *M. marinum* growth in the zebrafish infection model. The broad range of functions that scavenger receptors have is not only a result of the many ligands that they recognise, but also of the various co-receptors that they partner with. This combination enables them to mount a highly versatile response. The fact that CD14, one of the co-receptors of MARCO that has been proposed to aid in the cytokine response regulation, is missing in zebrafish highlights the necessity of future work to unravel the signal transduction pathway associated with Marco in zebrafish.

Acknowledgements

We thank Julien Rougeot for help with RNA deep sequencing analysis, and other group members for helpful discussions. We further thank Steven Renshaw (University of Sheffield) for the *Tg(mpx:GFP)* line, George Lutfalla (University Montpellier 2) for the *Tg(mpeg1:mCherry)* line, Graham Lieschke (Monash University) for the *Tg(mpeg1:EGFP)* and *Tg(mpeg1:Gal4-VP16)* lines, Anna Huttenlocher (University of Wisconsin) for L-plastin Ab, Astrid van der Sar (VU Medical Center, Amsterdam) for bacterial strains and plasmids, and Alex Nezhinsky and Fons Verbeek for making their Pixel count software available prior to publication. This work was supported by the Smart Mix Program of the Netherlands Ministry of Economic Affairs and the Ministry of Education, Culture and Science.

References

1. Murphy, J.E., Tedbury, P.R., Homer-Vanniasinkam, S., Walker, J.H. & Ponnambalam, S. Biochemistry and cell biology of mammalian scavenger receptors. *Atherosclerosis* **182**, 1-15 (2005).

2. Goldstein, J.L., Ho, Y.K., Basu, S.K. & Brown, M.S. Binding site on macrophages that mediates uptake and degradation of acetylated low density lipoprotein, producing massive cholesterol deposition. *Proc Natl Acad Sci U S A* **76**, 333-337 (1979).

3. Kzhyshkowska, J., Neyen, C. & Gordon, S. Role of macrophage scavenger receptors in atherosclerosis. *Immunobiology* **217**, 492-502 (2012).

4. Dorrington, M.G. *et al.* MARCO is required for TLR2- and Nod2-mediated responses to Streptococcus pneumoniae and clearance of pneumococcal colonization in the murine nasopharynx. *Journal of immunology* **190**, 250-258 (2013).

5. Pollock, S. *et al.* Uptake and trafficking of liposomes to the endoplasmic reticulum. *Faseb J* **24**, 1866-1878 (2010).

6. Xu, S. *et al.* Apolipoproteins of HDL can directly mediate binding to the scavenger receptor SR-BI, an HDL receptor that mediates selective lipid uptake. *Journal of lipid research* **38**, 1289-1298 (1997).

7. Emi, M. *et al.* Structure, organization, and chromosomal mapping of the human macrophage scavenger receptor gene. *J Biol Chem* **268**, 2120-2125 (1993).

8. Krieger, M. & Herz, J. Structures and functions of multiligand lipoprotein receptors: macrophage scavenger receptors and LDL receptor-related protein (LRP). *Annu Rev Biochem* **63**, 601-637 (1994).

9. Elomaa, O. *et al.* Cloning of a novel bacteria-binding receptor structurally related to scavenger receptors and expressed in a subset of macrophages. *Cell* **80**, 603-609 (1995).

10. Kraal, G., van der Laan, L.J., Elomaa, O. & Tryggvason, K. The macrophage receptor MARCO. *Microbes Infect* **2**, 313-316 (2000).

11. Palecanda, A. *et al.* Role of the scavenger receptor MARCO in alveolar macrophage binding of unopsonized environmental particles. *J Exp Med* **189**, 1497-1506 (1999).

12. van der Laan, L.J. *et al.* Macrophage scavenger receptor MARCO: in vitro and in vivo regulation and involvement in the anti-bacterial host defense. *Immunol Lett* **57**, 203-208 (1997).

13. van der Laan, L.J. *et al.* Regulation and functional involvement of macrophage scavenger receptor MARCO in clearance of bacteria in vivo. *J Immunol* **162**, 939-947 (1999).

14. Granucci, F. *et al.* The scavenger receptor MARCO mediates cytoskeleton rearrangements in dendritic cells and microglia. *Blood* **102**, 2940-2947 (2003).

15. Wermeling, F. *et al.* Class A scavenger receptors regulate tolerance against apoptotic cells, and autoantibodies against these receptors are predictive of systemic lupus. *J Exp Med* **204**, 2259-2265 (2007).

16. Rogers, N.J. *et al.* A defect in Marco expression contributes to systemic lupus erythematosus development via failure to clear apoptotic cells. *J Immunol* **182**, 1982-1990 (2009).

17. Tas, S.W., Quartier, P., Botto, M. & Fossati-Jimack, L. Macrophages from patients with SLE and rheumatoid arthritis have defective adhesion in vitro, while only SLE macrophages have impaired uptake of apoptotic cells. *Ann Rheum Dis* **65**, 216-221 (2006).

18. Podack, E.R., Deyev, V. & Shiratsuchi, M. Pore formers of the immune system. *Adv Exp Med Biol* **598**, 325-341 (2007).

19. Bowdish, D.M. *et al.* Genetic variants of MARCO are associated with susceptibility to pulmonary tuberculosis in a Gambian population. *BMC Med Genet* **14**, 47 (2013).

20. Ma, M.J. *et al.* Genetic variants in MARCO are associated with the susceptibility to pulmonary tuberculosis in Chinese Han population. *PLoS One* **6**, e24069 (2011).

21. Vergne, I., Chua, J., Singh, S.B. & Deretic, V. Cell biology of mycobacterium tuberculosis phagosome. *Annu Rev Cell Dev Biol* **20**, 367-394 (2004).

22. Bonilla, D.L. *et al.* Autophagy regulates phagocytosis by modulating the expression of scavenger receptors. *Immunity* **39**, 537-547 (2013).

23. Bowdish, D.M. *et al.* MARCO, TLR2, and CD14 are required for macrophage cytokine responses to mycobacterial trehalose dimycolate and Mycobacterium tuberculosis. *PLoS Pathog* **5**, e1000474 (2009).

24. Tobin, D.M. & Ramakrishnan, L. Comparative pathogenesis of Mycobacterium marinum and Mycobacterium tuberculosis. *Cellular microbiology* **10**, 1027-1039 (2008).

25. Parikka, M. *et al.* Mycobacterium marinum causes a latent infection that can be reactivated by gamma irradiation in adult zebrafish. *PLoS pathogens* **8**, e1002944 (2012).

26. Swaim, L.E. *et al.* Mycobacterium marinum Infection of Adult Zebrafish Causes Caseating Granulomatous Tuberculosis and Is Moderated by Adaptive Immunity. *Infection and Immunity* **74**, 6108-6117 (2006).

27. Clay, H. *et al.* Dichotomous Role of the Macrophage in Early Mycobacterium marinum Infection of the Zebrafish. *Cell Host & Microbe* **2**, 29-39 (2007).

28. Tobin, D.M. *et al.* The lta4h Locus Modulates Susceptibility to Mycobacterial Infection in Zebrafish and Humans. *Cell* **140**, 717-730 (2010).

29. van der Vaart, M., van Soest, J.J., Spaink, H.P. & Meijer, A.H. Functional analysis of a zebrafish myd88 mutant identifies key transcriptional components of the innate immune system. *Dis Model Mech* **6**, 841-854 (2013).

30. Cambier, C.J. *et al.* Mycobacteria manipulate macrophage recruitment through coordinated use of membrane lipids. *Nature* **505**, 218-222 (2014).

31. Zakrzewska, A. *et al.* Macrophage-specific gene functions in Spi1-directed innate immunity. *Blood* **116**, e1-11 (2010).

32. Wittamer, V., Bertrand, J.Y., Gutschow, P.W. & Traver, D. Characterization of the mononuclear phagocyte system in zebrafish. *Blood* **117**, 7126-7135 (2011).

33. Ellett, F., Pase, L., Hayman, J.W., Andrianopoulos, A. & Lieschke, G.J. mpeg1 promoter transgenes direct macrophage-lineage expression in zebrafish. *Blood* **117**, e49-e56 (2010).

34. Bernut, A. *et al.* Mycobacterium abscessus cording prevents phagocytosis and promotes abscess formation. *Proc Natl Acad Sci U S A* **111**, E943-952 (2014).

35. Renshaw, S.A. *et al.* A transgenic zebrafish model of neutrophilic inflammation. *Blood* **108**, 3976-3978 (2006).

36. Gray, C. *et al.* Simultaneous intravital imaging of macrophage and neutrophil behaviour during inflammation using a novel transgenic zebrafish. *Thromb Haemost* **105**, 811-819 (2011).

37. d'Alençon, C.A. *et al.* A high-throughput chemically induced inflammation assay in zebrafish. *BMC Biology* **8**, 151 (2010).

38. van der Sar, A.M. *et al.* Mycobacterium marinum Strains Can Be Divided into Two Distinct Types Based on Genetic Diversity and Virulence. *Infection and Immunity* **72**, 6306-6312 (2004).

39. van der Sar, A.M. *et al.* Zebrafish embryos as a model host for the real time analysis of Salmonella typhimurium infections. *Cellular Microbiology* **5**, 601-611 (2003).

40. Kimmel, C.B., Ballard, W.W., Kimmel, S.R., Ullmann, B. & Schilling, T.F. Stages of embryonic development of the zebrafish. *Dev Dyn* **203**, 253-310 (1995).

41. Benard, E.L. *et al.* Infection of zebrafish embryos with intracellular bacterial pathogens. *J Vis Exp* **61** pii: 3781. doi: 10.3791/3781 (2012).

42. Rougeot, J. *et al.* RNA sequencing of FACS-sorted immune cell populations from zebrafish infection models to identify cell specific responses to intracellular pathogens. *Methods in Molecular Biology* (In press).

43. Stockhammer, O.W., Zakrzewska, A., Hegedus, Z., Spaink, H.P. & Meijer, A.H. Transcriptome profiling and functional analyses of the zebrafish embryonic innate immune response to Salmonella infection. *J Immunol* **182**, 5641-5653 (2009).

44. Veneman, W.J. *et al.* A zebrafish high throughput screening system used for Staphylococcus epidermidis infection marker discovery. *BMC Genomics* **14**, 255 (2013).

45. Cui, C. *et al.* Infectious disease modeling and innate immune function in zebrafish embryos. *Methods Cell Biol* **105**, 273-308 (2011).

46. Schindelin, J. *et al.* Fiji: an open-source platform for biological-image analysis. *Nat Methods* **9**, 676-682 (2012).

47. Nezhinsky A.E., V.F.J. Efficient and Robust Shape Retrieval from Deformable Templates. *International Symposium on Leveraging Applications of Formal Methods* Part II, LNCS 7610 (T. Margaria, B. Steffen, and M. Merten (Eds.)), 42-55 (2012).

48. Elomaa, O. *et al.* Structure of the human macrophage MARCO receptor and characterization of its bacteria-binding region. *J Biol Chem* **273**, 4530-4538 (1998).

49. Kanwal, Z. *et al.* Deficiency in hematopoietic phosphatase ptpn6/Shp1 hyperactivates the innate immune system and impairs control of bacterial infections in zebrafish embryos. *J Immunol* **190**, 1631-1645 (2013).

50. Mathias, J.R. *et al.* Live imaging of chronic inflammation caused by mutation of zebrafish Hai1. *Journal of Cell Science* **120**, 3372-3383 (2007).

51. Yang, C.T. *et al.* Neutrophils exert protection in the early tuberculous granuloma by oxidative killing of mycobacteria phagocytosed from infected macrophages. *Cell Host Microbe* **12**, 301-312 (2012).

52. Colucci-Guyon, E., Tinevez, J.Y., Renshaw, S.A. & Herbomel, P. Strategies of professional phagocytes in vivo: unlike macrophages, neutrophils engulf only surface-associated microbes. *Journal of Cell Science* **124**, 3053-3059 (2011).

53. Sharif, O. *et al.* The scavenger receptor CD36 downmodulates the early inflammatory response while enhancing bacterial phagocytosis during pneumococcal pneumonia. *J Immunol* **190**, 5640-5648 (2013).

54. Benard, E.L. *et al.* The macrophage-expressed perforins Mpeg1 and Mpeg1.2 have anti-bacterial function in zebrafish. *Journal of Innate Immunity* (In press).

55. Akitake, C.M., Macurak, M., Halpern, M.E. & Goll, M.G. Transgenerational analysis of transcriptional silencing in zebrafish. *Developmental biology* **352**, 191-201 (2011).

56. Pisharath, H. & Parsons, M.J. Nitroreductase-mediated cell ablation in transgenic zebrafish embryos. *Methods Mol Biol* **546**, 133-143 (2009).

57. Davis, J.M. *et al.* Real-time visualization of mycobacterium-macrophage interactions leading to initiation of granuloma formation in zebrafish embryos. *Immunity* **17**, 693-702 (2002).

58. Hirsch, C.S., Ellner, J.J., Russell, D.G. & Rich, E.A. Complement receptor-mediated uptake and tumor necrosis factor-alpha-mediated growth inhibition of Mycobacterium tuberculosis by human alveolar macrophages. *J Immunol* **152**, 743-753 (1994).

59. Schlesinger, L.S., Bellinger-Kawahara, C.G., Payne, N.R. & Horwitz, M.A. Phagocytosis of Mycobacterium tuberculosis is mediated by human monocyte complement receptors and complement component C3. *J Immunol* **144**, 2771-2780 (1990).

60. Schlesinger, L.S. Macrophage phagocytosis of virulent but not attenuated strains of Mycobacterium tuberculosis is mediated by mannose receptors in addition to complement receptors. *J Immunol* **150**, 2920-2930 (1993).

61. Schlesinger, L.S., Hull, S.R. & Kaufman, T.M. Binding of the terminal mannosyl units of lipoarabinomannan from a virulent strain of Mycobacterium tuberculosis to human macrophages. *J Immunol* **152**, 4070-4079 (1994).

62. Schlesinger, L.S., Kaufman, T.M., Iyer, S., Hull, S.R. & Marchiando, L.K. Differences in mannose receptor-mediated uptake of lipoarabinomannan from virulent and attenuated strains of Mycobacterium tuberculosis by human macrophages. *J Immunol* **157**, 4568-4575 (1996).

63. Nakata, T. *et al.* CD14 directly binds to triacylated lipopeptides and facilitates recognition of the lipopeptides by the receptor complex of Toll-like receptors 2 and 1 without binding to the complex. *Cellular microbiology* **8**, 1899-1909 (2006).

64. Brightbill, H.D. *et al.* Host defense mechanisms triggered by microbial lipoproteins through toll-like receptors. *Science* **285**, 732-736 (1999).

65. Manukyan, M. *et al.* Binding of lipopeptide to CD14 induces physical proximity of CD14, TLR2 and TLR1. *Eur J Immunol* **35**, 911-921 (2005).

66. Iliev, D.B., Roach, J.C., Mackenzie, S., Planas, J.V. & Goetz, F.W. Endotoxin recognition: in fish or not in fish? *FEBS Lett* **579**, 6519-6528 (2005).

67. Meijer, A.H. *et al.* Expression analysis of the Toll-like receptor and TIR domain adaptor families of zebrafish. *Molecular immunology* **40**, 773-783 (2004).

68. Ribeiro, C.M., Hermsen, T., Taverne-Thiele, A.J., Savelkoul, H.F. & Wiegertjes, G.F. Evolution of recognition of ligands from Gram-positive bacteria: similarities and differences in the TLR2-mediated response between mammalian vertebrates and teleost fish. *Journal of immunology* **184**, 2355-2368 (2010).

69. Chen, Y. *et al.* A regulatory role for macrophage class A scavenger receptors in TLR4-mediated LPS responses. *Eur J Immunol* **40**, 1451-1460 (2010).

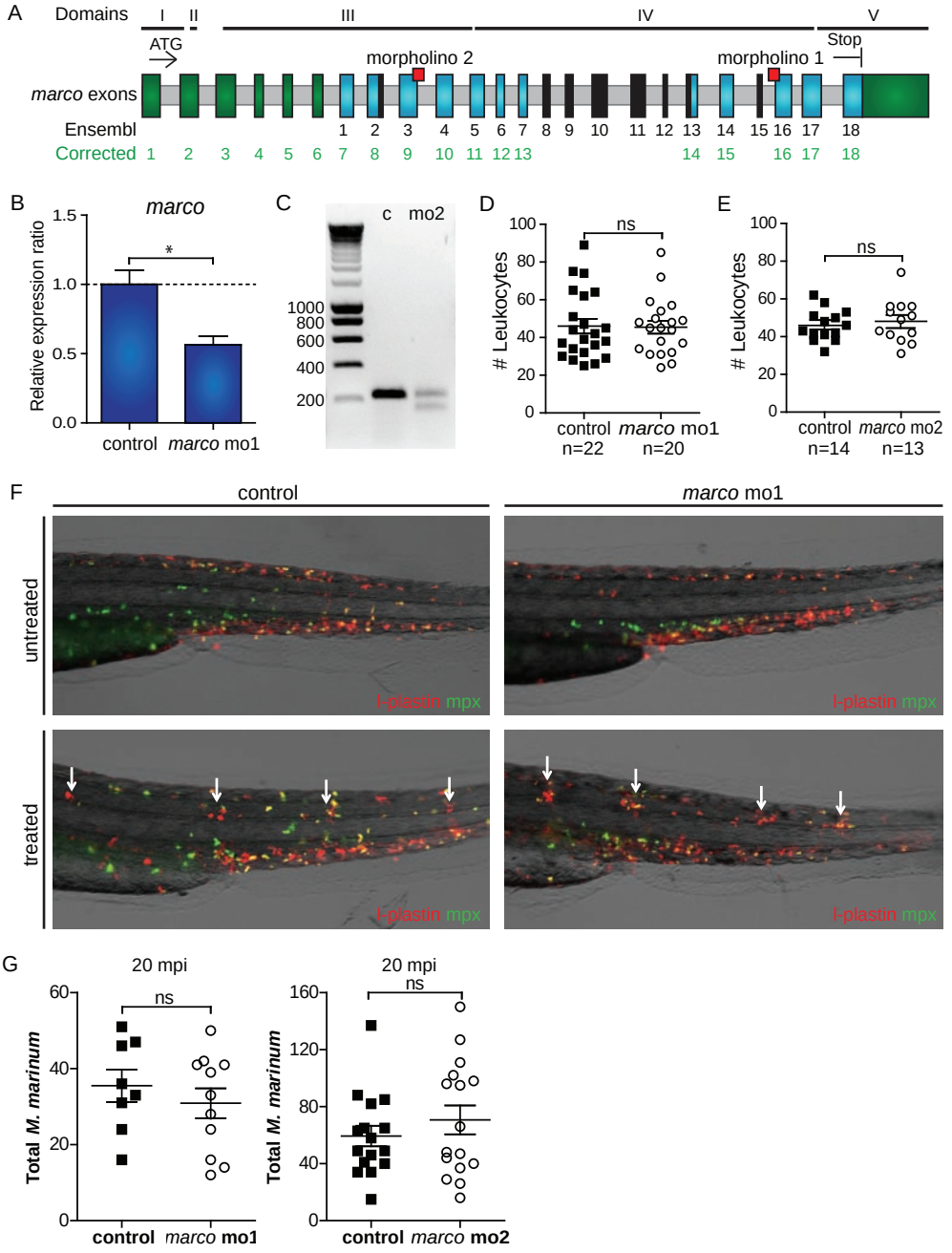

Supplementary figure 1. Validation of morpholino knockdown. (A) Corrected annotation of *marco* exons. The sequenced cDNA clone of *marco* shows that there are 6 additional exons (shown in green) prior to exon 1 in the current annotation in Ensembl (Zv9, ENSDARG00000059294), which was based on a predicted gene, LOC571584. Furthermore, the cDNA shows partial absence of Ensembl exons 2 and 13 and complete absence of exons 8 – 12 and 15 (shown in black), and an extended final exon (shown in green). Exons that are not different between the

Supplementary figure 1 continued: Ensembl annotation and the corrected annotation are shown in blue and introns are shown in grey. Exon-intron boundary sites targeted by morpholinos (red squares), the ATG and stop codon sites, and the conserved protein domains (I to V corresponding with fig. 1) are indicated. (B-C) Knockdown of *marco*. The predicted effect of splice blocking morpholinos 1 is deletion of exon 16 in the collagenous domain and the predicted effect of morpholino 2 is deletion of exon 9 in the spacer domain. The exon deletion effect of morpholino 1 could not be confirmed by RT-PCR, but qPCR analysis (28 hpf) demonstrated that the *marco* mRNA level was effectively reduced (B). Deletion of exon 9 following knockdown of *marco* with morpholino 2 was confirmed by RT-PCR (C) using RNA from embryos injected with *marco* morpholino 2 (mo2) or control morpholino (c). The expected RT-PCR product size for the control embryos is 228 bp and for *marco* mo2 morphants is 143 bp. (D-E) Normal leukocyte numbers in *marco* morphants. *marco* (D) morpholino 1 and (E) morpholino 2 morphants and control embryos were fixed at 30 hpf and were immuno-labelled with Ab against the general leukocyte marker L-plastin. Leukocyte numbers were counted blinded over the Duct of Cuvier, (ns = not significant). (F) Marco does not affect migration of leukocytes towards local inflammation sites. Representative images of copper sulphate treated control and *marco* morphant 3 dpf embryos. Embryos were immuno-labelled with Ab against the general leukocyte marker L-plastin (red signal) in combination with a neutrophil-specific Mpx TSA-staining (green signal) at 3 dpf. White arrows indicate accumulation of leukocytes at the local inflammation sites at the neuromasts. (G) Total number of *M. marinum* counted over Duct of Cuvier at 20 mpi for *marco* mo1 and mo2 morphants.

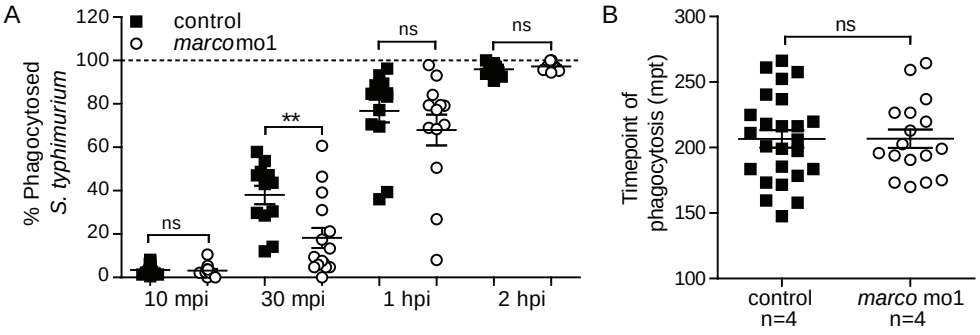

Supplementary figure 2. *marco* knockdown affects phagocytosis of *S. typhimurium* but not phagocytosis of dead cells. (A) An injected dose of 180 cfu of Ds-Red labelled *S. typhimurium* SL1027 is completely phagocytosed in wild type embryos at 2 hpi and *marco* knockdown leads to a delay in phagocytosis at 30 mpi. Each data point represents the percentage of phagocytosed *S. typhimurium* in an individual embryo and the mean ± SEM is indicated. (B) Phagocytosis of dead cells by healthy macrophages was not affected by knockdown of *marco.* Phagocytosis events of chemically ablated macrophages by healthy macrophages were quantified from time lapse movies of 4 embryos per group (representative images in fig. 3). Each data point represents a single phagocytosis event and the mean ± SEM is indicated.

Supplementary table 1. Zebrafish Marco homology compared to murine and human MARCO

A Protein homology

Identical / Similar	z-Marco	m-MARCO	h-MARCO
z-Marco	**100**	35	32
m-MARCO	62	**100**	66
h-MARCO	64	84	**100**

B Cysteine-rich domain V homology

Identical / Similar	z-Marco	m-MARCO	h-MARCO
z-Marco	**100**	52	50
m-MARCO	84	**100**	70
h-MARCO	86	90	**100**

***** Homology for (A) whole protein sequences and (B) Cysteine-rich domain V was determined between zebrafish Marco (z-Marco), murine MARCO (m-MARCO) and human MARCO (h-MARCO).

Supplementary table 2. Comparison of expression levels of selected infection inducible genes

			control uninf vs control inf		marco inf vs control inf	
Ensembl ID	**Description**	**Gene name**	**fold change**	**Adj P-value**	**fold change**	**Adj P-value**
ENSDARG00000059741	alpha-kinase 1	*alpk1*	2.8	0.00	0.9	1
ENSDARG00000007823	activating transcription factor 3	*atf3*	2.6	0.04	0.9	1
ENSDARG00000057121	complement component 7	*c7 (2 of 2)*	3.5	6.1E-05	0.6	0.38
ENSDARG00000086869	three-finger protein 5 (LOC100003647 precursor)	*cabz01040055.1*	16.0	3.2E-17	1.7	0.38
ENSDARG00000038025	chromobox homolog 7a	*cbx7a*	2.6	0.00	1.1	1
ENSDARG00000086654	Uncharacterized protein	*ct027762.4*	50.1	2.3E-21	0.8	1
ENSDARG00000075045	chemokine (C-X-C motif) ligand c1c	*cxcl-c1c*	16.8	8.9E-08	1.7	0.88
ENSDARG00000026039	cytochrome P450, family 1, subfamily A	*cyp1a*	13.3	2.1E-22	0.4	0.01
ENSDARG00000070420	cytochrome P450, family 24, subfamily A, polypeptide 1	*cyp24a1*	4.3	2.3E-07	0.4	0.01
ENSDARG00000092858	non-coding RNA	*fd36h06*	4.7	5.5E-06	1.3	1
ENSDARG00000053227	hepcidin antimicrobial peptide 2	*hamp2*	40.5	2.7E-13	1.2	1
ENSDARG00000027529	heme oxygenase (decycling) 1	*hmox1*	4.6	3.1E-07	0.2	1.6E-09
ENSDARG00000051912	hemopexin	*hpx (1 of 2)*	18.8	1.9E-30	1.0	1
ENSDARG00000093303	interferon induced transmembrane protein 10	*ifitm10*	2.3	0.09	1.7	0.49
ENSDARG00000014947	insulin-like growth factor binding protein 1a	*igfbp1a*	3.1	0.00	1.0	1
ENSDARG00000005419	interleukin 1, beta	*il1b*	10.5	0.00	1.3	1
ENSDARG00000053131	interleukin-1 receptor-associated kinase 3	*irak3*	26.9	2.9E-08	1.3	1
ENSDARG00000003523	intelectin 3	*itln3*	19.7	5.6E-26	0.6	0.60
ENSDARG00000033227	leukocyte cell-derived chemotaxin 2 like	*lect2l*	11.1	2.2E-22	1.2	1
ENSDARG00000090557	microfibrillar-associated protein 4	*mfap4 (6 of 13)*	62.8	5.6E-26	0.7	1
ENSDARG00000012395	matrix metalloproteinase 13a	*mmp13a*	6.3	5.5E-06	2.0	0.09
ENSDARG00000042816	matrix metalloproteinase 9	*mmp9*	19.4	1.4E-28	2.1	0.02
ENSDARG00000031136	monooxygenase, DBH-like 1	*moxd1*	5.1	0.00	2.6	0.00
ENSDARG00000074322	olfactomedin 4	*olfn4 (3 of 8)*	6.1	6.1E-06	0.3	0.01
ENSDARG00000016188	strawberry notch homolog 2 (Drosophila)	*sbno2 (2 of 3)*	2.2	0.04	1.1	1
ENSDARG00000092826	non-coding RNA	*si:ch211-243g18.3*	0.9	1	19.2	0.06
ENSDARG00000090352	non-coding RNA	*si:dkey-97i18.5*	34.9	1.4E-39	1.5	1
ENSDARG00000059805	solute carrier family 25, member 38a	*slc25a38a*	3.8	0.08	0.6	1
ENSDARG00000055252	synaptosomal-associated protein, 23kDa	*snap23 (2 of 2)*	4.2	0.01	1.5	1
ENSDARG00000055901	steap family member 4	*steap4*	2.7	0.00	2.0	0.03
ENSDARG00000007344	titin-cap (telethonin)	*tcap*	4.0	2.6E-06	2.2	0.01
ENSDARG00000075261	tissue inhibitor of metalloproteinase 2b	*timp2b*	3.5	3.8E-05	2.3	0.00

* All genes differentially regulated in *marco* infected morphants compared to infected control embryos (adjusted P-value <0.1) showed no significant change in uninfected *marco* morphants compared to uninfected control embryos with exception of *steap4* (fold change 2.1, adjusted P-value 0.04).